Sliding Mode Control for a Class of Control-Affine Nonlinear Systems

Belem Saldivar *,** **Juan Carlos Ávila Vilchis** *,⋆
Adriana H. Vilchis González * **Edgar Martínez Marbán** *

* *Facultad de Ingeniería - Universidad Autónoma del Estado de México, Instituto Literario No. 100 Ote., 50130 Toluca, Edo. de México, Mexico (e-mail: mbsaldivarma@conacyt.mx, jcavilav@uaemex.mx, avilchisg@uaemex.mx, edgmarb.08@gmail.com)*
** *Cátedras CONACYT, Av. Insurgentes Sur 1582, Col. Crédito Constructor, Del. Benito Juárez 03940 Ciudad de México, Mexico.*

Abstract: This paper concerns the synthesis of a sliding mode-based controller for a class of nonlinear control-affine systems where sufficient conditions for the system stabilization are provided. The effectiveness of the proposed approach is highlighted through a practical example: the regulation task of an aerodynamic system.

Keywords: Sliding mode control, nonlinear systems, stability conditions, aerodynamic system.

1. INTRODUCTION

The Sliding Mode Control (SMC) technique was introduced in the 1950s in the former Soviet Union as a variable structure control system (Emelyanov (1967)); two decades later, a book by Itkis (1976) and a survey paper by Utkin (1977) were published in English. Since then, several research studies were performed both from theoretical and practical perspectives, see for example DeCarlo et al. (1988), Hung et al. (1993) and Utkin (1978), where the fundamental principles of the SMC theory can be found, see also Azar and Zhu (2015), Bandyopadhyay et al. (2013), Bartolini et al. (2008), Fridman et al. (2012) and Pisano and Usai (2011) where recent results on SMC are summarized.

It is important to point out that a wide range of control problems in engineering have been treated using the SMC framework, just to mention some of them: Young et al. (1999) provides an overview of the problems arising in the practical implementation of the SMC technique, Bartolini et al. (2003) studies the SMC approach applied to mechanical systems, Piltan and Sulaiman (2012) and Othman et al. (2015) present a review of the application of SMC to robotic manipulators, and to electrohydraulic systems, respectively, Rossomando et al. (2014) applies the SMC technique to tackle the trajectory tracking problem in a mobile robot, Sefriti et al. (2012) propose a sliding mode based control for the robust tracking of a electrically-driven two-links robot manipulator, Rekioua et al. (2013) and Gonzalez Montoya et al. (2016) deal with the control of renewable energy generation systems via the SMC technique, Zhenga et al. (2014) and Khebbache and Tadjine (2013) present the SMC approach applied to quadrotor helicopters.

One can see that the SMC technique has been studied and applied, in distinct contexts, since its beginning to the present day. One of the reasons of the great success of the SMC approach is its robustness; with this kind of controllers, the system states are forced to reach and move through a predefined sliding surface, hence the system dynamics are determined by this surface instead of being influenced by uncertainties or disturbances. Once the sliding surface and the switching function are chosen, the dynamic performance of the system is fixed (Liu and Li (2014)). Besides robustness, the sliding mode controllers feature other remarkable properties such as accuracy and easy tuning and implementation.

This control method has been examined for a wide spectrum of system types including nonlinear systems, multi-input/multi-output systems, discrete-time models, large-scale and infinite-dimensional systems, and stochastic systems (Hung et al. (1993)). Furthermore, the control objectives have been extended from stabilization to other functions.

This paper concerns the stabilization via the SMC technique of a special class of nonlinear systems which are affine in the control. As an application example, the regulation problem for a particular aerodynamic system is addressed.

Interest for the modeling and control of aerodynamic systems has been present for many years in research projects all around the world. Several researchers have studied different aerodynamic systems with different approaches; for instance Bouguerra et al. (2015) and Lopes et al. (2006) study pedestal aerodynamic systems; in Bouguerra et al. (2015) a fault tolerant control for a 2 DoF (Degrees of Freedom) aerodynamic system is proposed while Lopes et al. (2006) considers an aerodynamic system with 3 DoF for which a predictive control is synthesized; Balas (2007) focuses on the modeling and control of the position and the

⋆ Corresponding author.

yaw angle of a quadrotor system; Schreck and Robinson (2007) points out the difficulties to the exact computing of aerodynamic forces, due to the lack of mathematical models; Béjar et al. (2007) proposes an illustrative reading about different aerodynamic platforms and control approaches. Optimization techniques applied to the design of rotor blades and applications that consider aerodynamic systems evolving at high altitude are reported in Leusink et al. (2015) and in Mueller et al. (2004), respectively.

In this paper, a sliding mode controller for a particular class of nonlinear control-affine systems is synthesized and the results are applied to the Aerodynamic Angular System (AAS), shown in Fig. 1 consisting of the elements described below.

The pedestal (1) provides support to the AAS bar (2) defining a planar angular motion with respect to the pivot (3) where a viscous friction torque that opposes the angular motion of the bar is assumed. Two actuators (4) and (5) are located at the extremities of the bar and generate the lift forces F_1 and F_2 thanks to the aerodynamic effect of the corresponding propellers that rotate with angular velocities ω_1 and ω_2, respectively. These actuators correspond to direct current motors. The pivots (6) and (7) at the bar ends, enable actuators to remain upright continuously in such a way that the lift forces will be vertical all the time. If the two aerodynamic forces F_1 and F_2 have the same magnitude, the bar (2) will remain horizontal; a difference between these two aerodynamic forces will produce a torque with respect to the pivot (3) and, consequently, the rotation of the bar (2). As it is illustrated in Fig. 1, an offset (δ) is present in this system, so the bar does not rotate about its geometrical center; the bar rotation is, then, an asymmetrical motion. An angular motion sensor is located on the pivot (3) to measure the rotation angle of the bar (θ) and to deduce its angular velocity ($\dot{\theta}$).

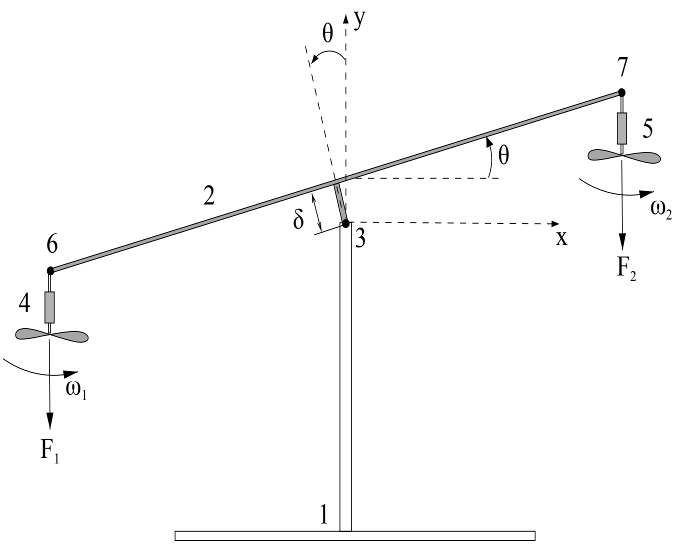

Fig. 1. Aerodynamic Angular System diagram.

This paper is organized as follows: Section 2 is devoted to the sliding mode control design for a class of nonlinear systems and sufficient conditions for the system stability are provided; in Section 3 the regulation problem statement for the AAS is provided, numerical results concerning the regulation via the SMC are discussed and the effectiveness of the proposed approach is pointed out; the paper concludes and describes directions for the future work in Section 4.

2. SLIDING MODE CONTROL

Consider a nth-order nonlinear system of the form: [1]

$$\dot{x} = Ax + \bar{f}(x) + \sum_{i=1}^{m} \bar{g}_i(x)u_i, \tag{1}$$

where $x \in \mathcal{R}^n$ is the state vector and $u_i \in \mathcal{R}$, $i = 1, ..., m$ are the control inputs. In the linear part, matrix $A \in \mathcal{R}^{n\times n}$ is given by:

$$A = \begin{bmatrix} 0 & 1 & 0 & \cdots & 0 \\ 0 & 0 & 1 & & 0 \\ \vdots & \vdots & & \ddots & \\ 0 & 0 & 0 & & 1 \\ -a_n & -a_{n-1} & -a_{n-2} & \cdots & -a_1 \end{bmatrix},$$

with constants $a_1, ..., a_n$. The drift and control vector fields $\bar{f}$ and $\bar{g}_i$, respectively, are such that:

$$\bar{f}(x) = \begin{bmatrix} 0 \\ 0 \\ \vdots \\ 0 \\ f(x) \end{bmatrix}, \quad \bar{g}_i(x) = \begin{bmatrix} 0 \\ 0 \\ \vdots \\ 0 \\ g_i(x) \end{bmatrix},$$

where $f(x)$ and $g_i(x)$ are scalar nonlinear functions.

It is well known that the sliding mode control technique drives the state of the system to a predefined surface allowing the reaching of the equilibrium. In general, this method consists of two elements: the switching rule and the equivalent control.

The switching law constitutes a discontinuous control which is applied in order to reach the sliding surface while the equivalent control is continuous and aims keeping the system state on the sliding surface. A sliding mode-based technique to control a nonlinear system of the form (1) is proposed in what follows. First of all, the switching part of the sliding mode control will be derived.

Consider a sliding surface defined by

$$S = Kx = 0, \quad K \in \mathcal{R}^{1\times n}, \tag{2}$$

where K is a row vector with constant elements.

The sliding surface is reached by the system state if the condition

$$S\dot{S} < 0$$

is fulfilled (see for instance Sira Ramírez (2015)); in view of (2), this condition is rewritten as

$$KxK\dot{x} < 0.$$

Introducing the system dynamics given by (1), one gets:

$$KxK(Ax + \bar{f}(x)) + \sum_{i=1}^{m} KxK\bar{g}_i(x)u_i < 0. \tag{3}$$

[1] In the following, the time dependence symbol (t) of dynamic variables will be omitted for simplification.

Inequality (3) is satisfied for a proper choice of u_i for all $i = 1, ..., m$.

Consider the following switching law:

$$u_{i_s} = \begin{cases} -\phi \frac{\left|KxK(Ax+\bar{f}(x))\right|}{KxK\bar{g}_i(x)} & \text{if } S \neq 0 \text{ and } KxK\bar{g}_i(x) \neq 0, \\ 0 & \text{else,} \end{cases} \tag{4}$$

where ϕ is a positive constant. Then, by taking

$$u_i = u_{i_s},$$

inequality (3) is reduced to:

$$KxK(Ax + \bar{f}(x)) - m\phi \left|KxK(Ax + \bar{f}(x))\right| < 0 \tag{5}$$

that is satisfied for all

$$\phi > 1/m.$$

Since $\frac{|Kx|}{Kx} = \mathrm{sgn}(Kx)$, the switching control (4) can be rewritten as follows:

$$u_{i_s} = \begin{cases} -\phi \mathrm{sgn}(Kx) \frac{\left|K(Ax+\bar{f}(x))\right|}{K\bar{g}_i(x)} & \text{if } S \neq 0 \text{ and } K\bar{g}_i(x) \neq 0, \\ 0 & \text{else,} \end{cases} \tag{6}$$

Remark 1. The robustness property against matched uncertainties of the switching control can be ensured by a proper choice of the controller gain ϕ. To see this, consider a system of the form:

$$\dot{x} = Ax + \bar{f}(x) + \sum_{i=1}^{m} \bar{g}_i(x)(u_i + \xi_i)$$

where ξ_i represents external disturbances or model uncertainties which are unknown but bounded in magnitude:

$$|\xi_i| \leq \bar{\xi}_i, \quad i = 1, ..., m,$$

with $\bar{\xi}_i$ known constant upper bounds.

Setting

$$\eta = \left|K(Ax + \bar{f}(x))\right|,$$

the reaching condition (RC) stated in (5) would be:

$$RC := KxK(Ax+\bar{f}(x)) - m\phi \left|Kx\right| \eta + \sum_{i=1}^{m} KxK\bar{g}_i(x)\xi_i < 0$$

Note that

$$RC \leq |Kx|\,\eta - m\phi\,|Kx|\,\eta + \sum_{i=1}^{m} |KxK\bar{g}_i(x)\xi_i|,$$

$$RC \leq \eta - m\phi\eta + \sum_{i=1}^{m} |K\bar{g}_i(x)|\,\bar{\xi}_i,$$

then, the reaching condition is satisfied for

$$\phi > \frac{1}{m} + \frac{1}{m\eta} \sum_{i=1}^{m} |K\bar{g}_i(x)|\,\bar{\xi}_i.$$

Next, the equivalent control will be derived. To guarantee that the system state remains on S during the sliding phase, the following condition must be satisfied:

$$\frac{d}{dt} S = 0 \quad \text{when} \quad S = 0. \tag{7}$$

Note that

$$\frac{d}{dt} S = K\dot{x} = K(Ax + \bar{f}(x)) + \sum_{i=1}^{m} K\bar{g}_i(x)u_i.$$

Thus, condition (7) is satisfied by considering the following equivalent control for $i = 1, ..., m$:

$$u_{i_{eq}} = \begin{cases} -\frac{1}{m} \frac{K(Ax+\bar{f}(x))}{K\bar{g}_i(x)} & \text{if } S = 0 \text{ and } K\bar{g}_i(x) \neq 0, \\ 0 & \text{else.} \end{cases} \tag{8}$$

So, the nonlinear system (1) can be controlled by the sliding mode control defined by:

$$u_i = u_{i_s} + u_{i_{eq}}, \tag{9}$$

where u_{i_s} and $u_{i_{eq}}$ are given by (6) and (8), respectively.

2.1 Stability analysis

The stability of the nonlinear system (1) under the sliding mode controller (9) depends on two stages: the reaching phase and the sliding mode. The stability of the closed loop system is guaranteed if the reaching condition is satisfied and the system remains stable on the sliding surface. The stability during the reaching phase is verified since $\dot{S}S < 0$ when $S \neq 0$, but it is necessary to guarantee the stability during the sliding mode.

On the sliding surface, the equality:

$$S = Kx = 0$$

holds. Let us set

$$x = \begin{bmatrix} x_a \\ x_n \end{bmatrix}, \quad x_a = \begin{bmatrix} x_1 \\ \vdots \\ x_{n-1} \end{bmatrix},$$

and

$$K = \begin{bmatrix} \bar{K} & 1 \end{bmatrix}, \quad \bar{K} = \begin{bmatrix} k_1 & k_2 & \cdots & k_{n-1} \end{bmatrix}.$$

Then, the equality $Kx = 0$ implies:

$$x_n = -\bar{K}x_a. \tag{10}$$

Regarding the above relation, the convergence of x_a to the zero equilibrium point can be proved trough the convergence of x_n.

From (1), one can obtain:

$$\dot{x}_n = -a_n x_1 - a_{n-1}x_2 - \cdots - a_1 x_n + f(x) + \sum_{i=1}^{m} g_i(x)u_i. \tag{11}$$

The control u_i on the sliding surface corresponds to the equivalent control (8), where:

$$K(Ax+\bar{f}(x)) = [k_1 \cdots k_{n-1} 1]\begin{bmatrix} x_2 \\ \vdots \\ x_n \\ -a_n x_1 - \cdots - a_1 x_n + f(x) \end{bmatrix}$$

$$= k_1 x_2 + \cdots + k_{n-1} x_n - a_n x_1 - a_{n-1} x_2 -$$

$$\cdots - a_1 x_n + f(x),$$

and

$$K\bar{g}_i(x) = g_i(x).$$

Substituting the equivalent control into (11) yields:

$$\begin{aligned} \dot{x}_n &= -k_1 x_2 - \cdots - k_{n-1} x_n \\ &= -k_1 x_2 - \cdots - k_{n-1}(-k_1 x_1 - \cdots - k_{n-1} x_{n-1}). \end{aligned} \tag{12}$$

Consider the Lyapunov function

$$V(x) = \frac{1}{2} x_n^2.$$

Note that

$$\dot{V}(x) = x_n \dot{x}_n,$$

which, in view of (10) and (12), can be written as

$$\dot{V}(x) = x_a^T \Psi x_a,$$

where Ψ is the symmetric matrix defined in (13) (next page). Then $\dot{V}(x) < 0$ is fulfilled for $k_1, \cdots, k_{n-1}$ satisfying $\Psi < 0$ and the system is stable during the sliding mode.

The above result is summarized in the following theorem.

Theorem 1. The nonlinear system (1) is stabilizable by the sliding mode control (9) with $\phi > 1/m$ and

$$K = [k_1 \cdots k_{n-1} \;\; 1],$$

where $k_1, k_2, ..., k_{n-1}$ are such that the matrix inequality $\Psi < 0$, with Ψ given in (13), is satisfied.

Remark 2. Note that for $n = 1$, the switching and the equivalent control are given by:

$$u_{i_s} = \begin{cases} -\phi \mathrm{sgn}(x) \frac{|-a_1 x + f(x))|}{g_i(x)} & \text{if } S \neq 0 \text{ and } g_i(x) \neq 0, \\ 0 & \text{else,} \end{cases}$$

$$u_{i_{eq}} = \begin{cases} -\frac{1}{m} \frac{-a_1 x + f(x)}{g_i(x)} & \text{if } S = 0 \text{ and } g_i(x) \neq 0, \\ 0 & \text{else.} \end{cases}$$

For $n = 2$, the condition on the controller gains is reduced to $-k_1^3 < 0$, i.e., $k_1 > 0$, and, for $n > 2$, it corresponds to a nonlinear matrix inequality which can be solved using an appropriate computational package such that the PENLAB of MATLAB.

3. PRACTICAL EXAMPLE: AERODYNAMIC ANGULAR SYSTEM REGULATION

The effectiveness of the proposed approach is highlighted through a practical example: the regulation problem for the AAS described in Section 1.

3.1 AAS model

The regulation problem for this system consists on driving the angle θ defined by the rotation of the bar (see Fig. 1) to a predefined constant reference value θ_{ref} by controlling the lift forces F_1 and F_2. To achieve this goal, an accurate model of the AAS is required.

In Martínez Marbán (2015), a Lagrangian formulation is used to obtain the following model that represents the one degree of freedom dynamics of the AAS:

$$\dot{x} = Ax + \bar{f}(x) + \bar{g}_1(x)u_1 + \bar{g}_2(x)u_2, \tag{14}$$

where

$$x = \begin{bmatrix} x_1 \\ x_2 \end{bmatrix} = \begin{bmatrix} \theta \\ \dot{\theta} \end{bmatrix}, \quad A = \begin{bmatrix} 0 & 1 \\ 0 & \alpha_1 \end{bmatrix}, \quad \bar{f}(x) = \begin{bmatrix} 0 \\ f(x) \end{bmatrix},$$

$$f(x) = \alpha_2 \sin\theta, \quad \bar{g}_i(x) = \begin{bmatrix} 0 \\ g_i(x) \end{bmatrix},$$

$$g_1(x) = \alpha_3 \sin\theta + \alpha_4 \cos\theta, \quad g_2(x) = \alpha_3 \sin\theta - \alpha_4 \cos\theta.$$

The control inputs u_1 and u_2 correspond to the lift forces generated from the left and right propellers, respectively, and the constants α_i, $i = 1, ..., 4$ are defined by the parameters of the AAS.

Notice that this model constitutes a nonlinear system of the form (1). To tackle the regulation problem stated before, the results presented in Section 2 are applied.

3.2 Regulation task

In view of the application under consideration, the sliding surface is defined as follows:

$$S = Kx_s, \tag{15}$$

where

$$x_s = \begin{bmatrix} x_1 - x_1^* \\ x_2 \end{bmatrix} = \begin{bmatrix} \theta - \theta_{ref} \\ \dot{\theta} \end{bmatrix}.$$

In view of (15), the reaching condition is given by:

$$Kx_s K\dot{x}_s = Kx_s K\dot{x} < 0. \tag{16}$$

Then, from (16) and the system dynamics (14), the switching control (6) can be rewritten as:

$$u_{i_s} = \begin{cases} -\phi \mathrm{sgn}(Kx_s) \frac{|K(Ax+\bar{f}(x))|}{K\bar{g}_i(x)} & \text{if } S \neq 0 \text{ and } K\bar{g}_i(x) \neq 0, \\ 0 & \text{else.} \end{cases} \tag{17}$$

$$\Psi = \begin{bmatrix} -k_1^2 k_{n-1} & \frac{1}{2}k_1^2 - k_1 k_2 k_{n-1} & \frac{1}{2}k_1 k_2 - k_1 k_3 k_{n-1} & \cdots & \frac{1}{2}k_1 k_{n-2} - k_1 k_{n-1}^2 \\ * & k_1 k_2 - k_2^2 k_{n-1} & \frac{1}{2}k_2^2 - k_2 k_3 k_{n-1} + \frac{1}{2}k_1 k_3 & \cdots & \frac{1}{2}k_2 k_{n-2} - k_2 k_{n-1}^2 + \frac{1}{2}k_1 k_{n-1} \\ * & * & k_2 k_3 - k_3^2 k_{n-1} & \cdots & \frac{1}{2}k_3 k_{n-2} - k_3 k_{n-1}^2 + \frac{1}{2}k_2 k_{n-1} \\ \vdots & \vdots & \vdots & \ddots & \vdots \\ * & * & * & * & k_{n-2}k_{n-1} - k_{n-1}^3 \end{bmatrix}, \tag{13}$$

Following (8), the equivalent control is given by:

$$u_{i_{eq}} = \begin{cases} -\frac{1}{2}\frac{K(Ax+\bar{f}(x))}{K\bar{g}_i(x)} & \text{if } S = 0 \text{ and } K\bar{g}_i(x) \neq 0, \\ 0 & \text{else.} \end{cases} \tag{18}$$

It is concluded that the regulation problem for the AAS modeled by (14) can be solved through the application of the sliding mode control defined by (9) where u_{i_s} and $u_{i_{eq}}$ are given by (17) and (18), respectively.

Next, it will be shown that, for this study case, the stability condition stated in Theorem 1 is reduced to $k_1 > 0$.

Following the developments presented in Section 2, the control gain vector is chosen as:

$$K = [\,k_1 \;\; 1\,].$$

Then, on the sliding surface,

$$S = Kx_s = 0$$

implies

$$x_2 = -k_1(x_1 - x_1^*). \tag{19}$$

The following equation is derived from the system dynamics:

$$\dot{x}_2 = \alpha_1 x_2 + f(x) + g_1(x)u_1 + g_2(x)u_2.$$

Substituting the equivalent control (acting during the sliding mode) given by:

$$u_i = u_{i_{eq}} = -\frac{1}{2}\frac{k_1 x_2 + \alpha_1 x_2 + f(x)}{g_i(x)}, \tag{20}$$

yields

$$\dot{x}_2 = -k_1 x_2.$$

Consider the Lyapunov function

$$V(x) = \frac{1}{2}x_2^2,$$

observe that

$$\dot{V}(x) = x_2\dot{x}_2 = -k_1 x_2^2,$$

then $\dot{V}(x) < 0$ is satisfied for $k_1 > 0$.

3.3 Numerical results

In terms of the model parameters, for $K = [\,k_1 \;\; 1\,]$, the switching and the equivalent control can be written as follows:

$$u_{i_s} = \begin{cases} -\phi\frac{\gamma}{g_i} & \text{if } S \neq 0 \text{ and } g_i \neq 0, \\ 0 & \text{else,} \end{cases} \tag{21}$$

with $\phi > 1/2$ and

$$\gamma = \mathrm{sgn}((k_1(\theta - \theta_{ref}) + \dot{\theta}))\left|\dot{\theta}(k_1 + \alpha_1) + f\right|,$$

$$u_{i_{eq}} = \begin{cases} -\frac{1}{2}\frac{\dot{\theta}(k_1+\alpha_1)+f}{g_i} & \text{if } S = 0 \text{ and } g_i \neq 0, \\ 0 & \text{else.} \end{cases} \tag{22}$$

The numerical values of the proposed system parameters are given in Table 1. It is worth noting that these values are derived from physical characteristics of the system such as lengths, masses and friction coefficients that will not suffer variations while performing experiments once a prototype is built.

Table 1. AAS parameters.

Parameter	**Value**	**Units**
α_1	-0.01764	s^{-1}
α_2	0.4079	s^{-2}
α_3	-0.02352	$(kgm)^{-1}$
α_4	-1.435	$(kgm)^{-1}$

In this section one can notice that the regulation task is achieved for any controller gains such that $\phi > 1/2$ and $k_1 > 0$; however, the response velocity and the controllers size are directly related with the choice of ϕ and k_1.

Fig. 2 shows the evolution of the state for $\theta_{ref} = -5°$ and gains $\phi = 25$ and $k_1 = 0.2$. As one can see, the position of the AAS bar starts at the horizontal position with $x_1 = 0$ and then reaches the reference value, the variable x_2, corresponding to the angular velocity of the bar, exhibits the expected behavior: its magnitude increases allowing the regulation task and once the reference value is reached, it goes to zero. In this case, the angular velocity of the bar takes negative values before reaching the stable condition ($x_2 = 0$) since the reference is negative too.

The behavior of the control inputs u_1 and u_2, under the previous conditions ($\theta_{ref} = -5°$ and gains $\phi = 25$ and $k_1 = 0.2$), is shown in Fig. 3 where the chatter phenomenon, associated to this kind of strategy, is noted.

It is well known that the chattering problem in one of the main drawbacks of applying the sliding mode control

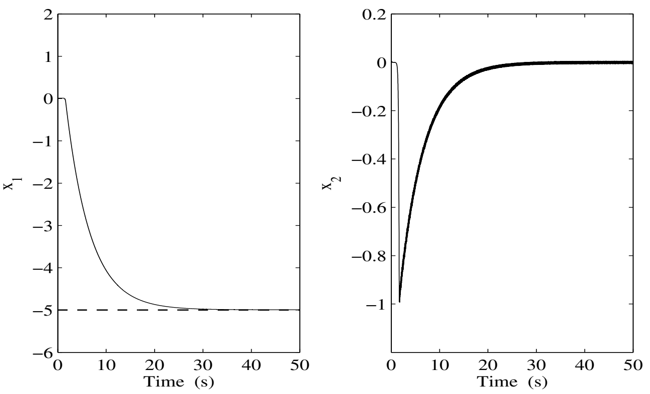

Fig. 2. Closed loop response of the AAS state with $\theta_{ref} = -5°$, $\phi = 25$ and $k_1 = 0.2$.

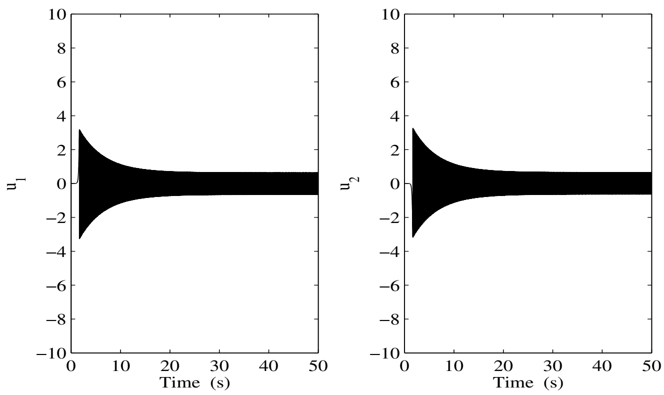

Fig. 3. Control behavior of the AAS with $\theta_{ref} = -5°$, $\phi = 25$ and $k_1 = 0.2$.

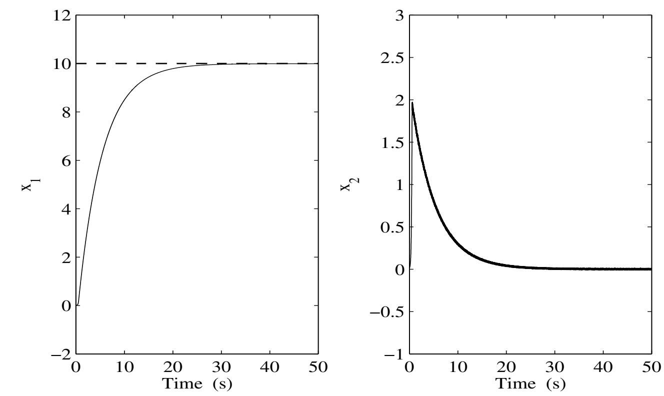

Fig. 4. Closed loop response of the AAS state with $\theta_{ref} = 10°$, $\phi = 25$ and $k_1 = 0.2$.

to real applications. From the control engineer's point of view, chattering is undesirable because it often causes control inaccuracy, high heat loss in electric circuitry, and high wear of moving mechanical parts (Wu et al. (2014)). Considerable research has been devoted to the chattering elimination/reduction problem; see for instance Bartoszewicz (2000), Lee et al. (2009), and Bendaas and Naceri (2013).

Theoretically, the ideal sliding mode implies infinite switching frequency (Utkin and Lee (2006)) so that the controlled variables can track a certain reference path to achieve the desired dynamic response and steady-state operation. However, in practice, an ideal sliding mode does not exist because the switching frequency of the control devices has a finite limit. In other words, there is no device that can switch to an infinite frequency (Bendaas and Naceri (2013)). Therefore one must implement a technique that guarantees a finite and possibly constant switching frequency. To do so, one can incorporate a constant ramp or timing function directly into the controller or use an adaptive hysteresis band (He et al. (2010), Tan et al. (2005)), among other approaches.

In the case under consideration, the infinite frequency chattering is triggered by the discontinuous term in the switching control (21). Since it switches between two structures during its operation, the control system undergoes oscillation near the sliding surface. A commonly used method to alleviate the chattering is to replace the discontinuous function by an "smoothing" term, as will be seen later in this section.

The next paragraphs are devoted to the numerical results obtained for a positive value reference $\theta_{ref} = 10°$ where the effectiveness of the strategy as well as the effect of the gains ϕ and k_1 on its performance are highlighted.

Fig. 4 illustrates the evolution of the states x_1 and x_2 for $\phi = 25$ and $k_1 = 0.2$; in the same way as for the case shown in Fig. 2, x_2 exhibits an expected behavior going through increasing and decreasing positive values before reaching zero that corresponds to the stable angular position of the bar.

A smaller value of the ϕ gain generates a slower response as it can be observed in Fig. 5, where stabilization is reached approximately ten seconds after what is reached with a higher gain value; here $\phi = 1.3$ is considered instead of 25, the other parameters remain invariant.

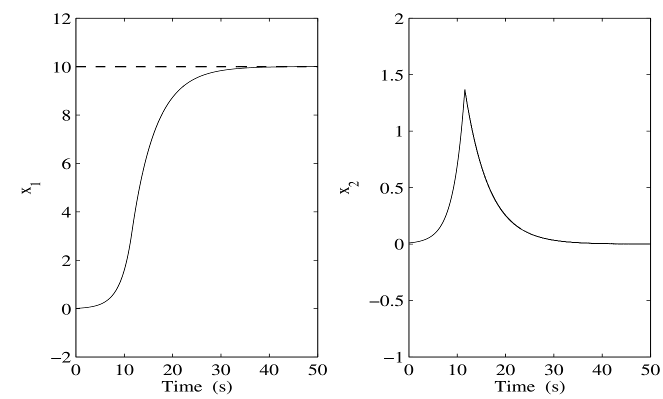

Fig. 5. Closed loop response of the AAS state with $\theta_{ref} = 10°$, $\phi = 1.3$ and $k_1 = 0.2$.

The behavior of the control inputs for the two choices illustrated previously are displayed in Fig. 6 where one can see that when $\phi = 1.3$ the controller takes about 10 seconds to start following the reference angle; however, the controllers magnitude is smaller compared to the case when $\phi = 25$.

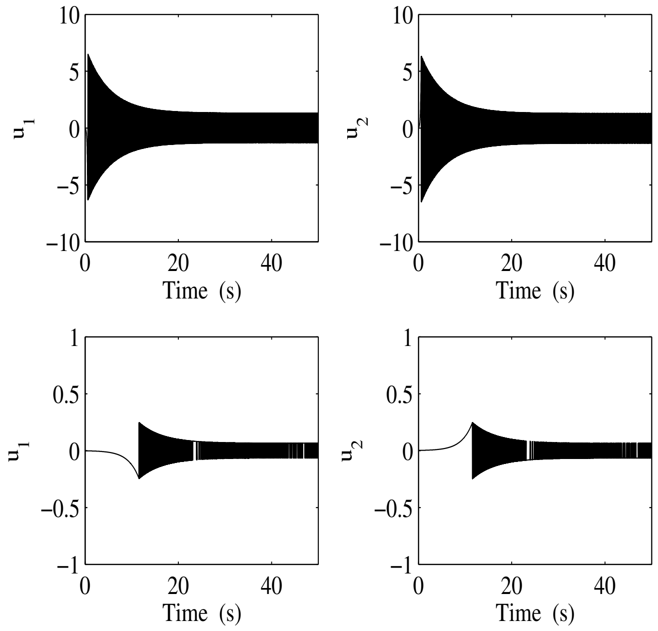

Fig. 6. Control signals with $\theta_{ref} = 10°$, $k_1 = 0.2$, $\phi = 25$ (top) and $\phi = 1.3$ (bottom).

Concerning the k_1 gain, Fig. 7 shows that the higher the value of k_1, the faster the system response. In this case, $\phi = 1.3$ and k_1 was increased from 0.2 to 3.2 allowing the convergence of the trajectories to the desired values in the first few seconds.

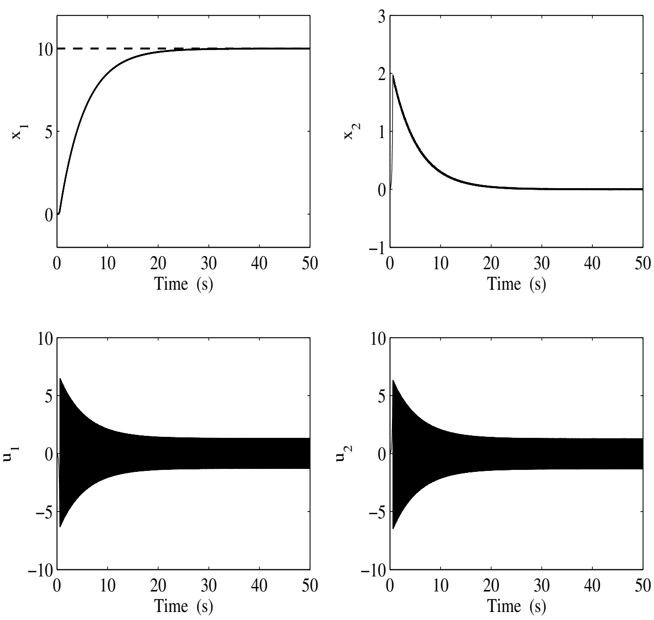

Fig. 7. Closed loop response of the AAS with $\theta_{ref} = 10°$, $\phi = 1.3$ and $k_1 = 3.2$; state behavior (top) and control behavior (bottom).

The observed results regarding the transient response of the system match the general idea that higher controller gains lead to faster system responses. However, it is important to considerate tradeoffs between goals in control design. *"Some of the tradeoffs ... are intuitively obvious: e.g., in mechanical systems, it takes larger actuator signals (forces, torques) to have faster responses..."* (Boyd (1991)).

In the case under consideration, the price paid for a higher speed of the response is a considerable increase in the controllers magnitude. In practice, the controllers size take importance due to the presence of physical limitations of the actuators in a real plant. Usually, it is required that the control inputs satisfy certain constraints related to its magnitude ($|u| < u_{max}$) to be implemented, then, an optimal trade-off between the required response velocity and the controller size must be established.

As discussed previously, the discontinuity associated with the nonlinear switching control is the main difficulty in a practical implementation, especially in mechanical systems. Usually, this has been avoided by "smoothing" the discontinuity. After doing this, the state trajectories no longer slide on the sliding surface, and instead they evolve in the vicinity of the sliding surface: this is termed as pseudo-sliding (Hamayun et al. (2016)).

The discontinuity can be avoided by using the following approximation:

$$\mathrm{sgn}(x) \approx \tanh(cx),$$

where c is a design scalar. Notice that as $c \to \infty$, the function $\tanh(cx)$ converges to the standard sign function.

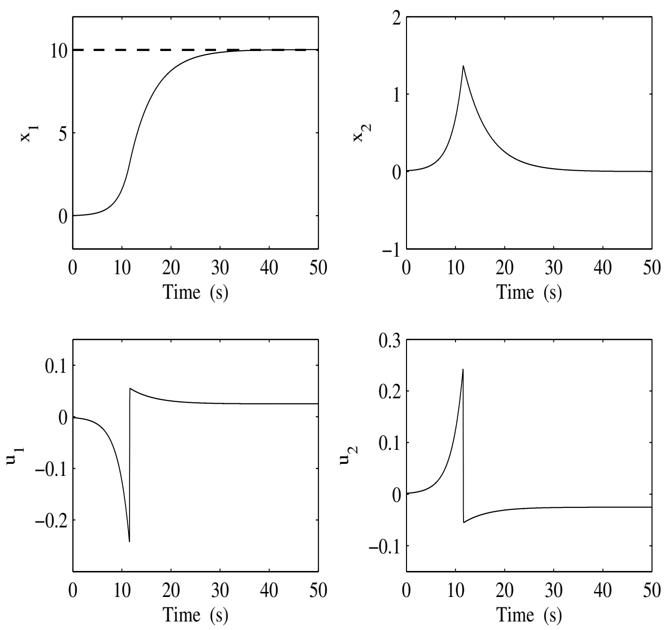

Fig. 8. Closed loop response of the AAS using a smooth approximation of the discontinuity with $c = 100$, $\theta_{ref} = 10°$, $\phi = 1.3$ and $k_1 = 0.2$.

Fig. 8 shows that the chattering or infinite frequency switching of the control signal has been eliminated by replacing the term $\mathrm{sgn}(Kx_s)$ by $\tanh(100Kx_s)$ in the switching control. Due to this approximation, the sliding motion will be in the vicinity of the sliding surface. As it is illustrated in Fig. 8, the state behaves in the same way that the response shown in Fig. 5.

4. CONCLUSIONS

In this paper a sliding mode control for a class of nonlinear control-affine systems is proposed. The strategy allows providing an efficient sliding mode control consisting of two elements: a switching control law which guarantees the system stability during the reaching phase, and an equivalent control law which aims at keeping the system state on the sliding surface once reached. The conditions on the controller gains for the closed loop system stability are formulated in terms of a nonlinear matrix inequality. The efficacy of the proposed approach was illustrated by tackling the regulation problem in the Aerodynamic Angular System; with this approach, the bar position can be driven to a prescribed angle through the manipulation of the lift forces generated by the aerodynamic effect in the system. An appropriate choice of the control gains allows adjusting the convergence rate and the controllers size.

Future work will be oriented to the construction of the Aerodynamic Angular System, to its electronic instrumentation, to the establishment of communication between the AAS and a computer and to perform several experimental test to validate the theoretical results presented in this paper. Besides, the trajectory tracking problem will be addressed.

REFERENCES

Azar, A.T. and Zhu, Q. (eds.) (2015). *Advances and applications in sliding mode control systems*, volume 576 of *Studies in Computational Intelligence*. Springer International Publishing.

Balas, C. (2007). *Modelling and linear control of a quadrotor*. Master's thesis, Cranfield University.

Bandyopadhyay, B., Janardhanan, S., and Spurgeon, S.K. (eds.) (2013). *Advances in sliding mode control: concept, theory and implementation*, volume 440 of *Lecture Notes in Control and Information Sciences*. Springer-Verlag Berlin Heidelberg.

Bartolini, G., Fridman, L., Pisano, A., and Usai, E. (eds.) (2008). *Modern sliding mode control theory: new perspectives and applications*, volume 375 of *Lecture Notes in Control and Information Sciences*. Springer-Verlag Berlin Heidelberg.

Bartolini, G., Pisano, A., E., P., and Usai, E. (2003). A survey of applications of second-order sliding mode control to mechanical systems. *A survey of applications of second-order sliding mode control to mechanical systems*, 76(9-10), 875–892.

Bartoszewicz, A. (2000). Chattering attenuation in sliding mode control systems. *Control and Cybernetics*, 29(2), 585–594.

Béjar, M., Ollero, A., and Cuesta, F. (2007). *Modeling and control of autonomous helicopters*, volume 353 of *Lecture Notes in Control and Information Sciences*. Springer Berlin Heidelberg.

Bendaas, I. and Naceri, F. (2013). A new method to minimize the chattering phenomenon in sliding mode control based on intelligent control for induction motor drives. *Serbian Journal of Electrical Engineering*, 10(2), 231–246.

Bouguerra, A., Saigaa, D., Kara, K., and Zeghlache, S. (2015). Fault-tolerant Lyapunov-gain-scheduled PID control of a quadrotor UAV. *International Journal of Intelligent Engineering and Systems*, 8(2), 1–6.

Boyd, S. (1991). *Linear controller design: limits of performance*. Prentice Hall.

DeCarlo, R., Zak, S., and Mathews, G. (1988). Variable structure control of nonlinear multivariable systems: a tutorial. *Proceedings of the IEEE*, 76(3), 212–232.

Emelyanov, S.V. (1967). *Variable structure control systems*. Moscow: Nauka (in Russian).

Fridman, L., Moreno, J., and Iriarte, R. (eds.) (2012). *Sliding modes after the first decade of the 21st century: state of the art*, volume 412 of *Lecture Notes in Control and Information Sciences*. Springer-Verlag Berlin Heidelberg.

Gonzalez Montoya, D., Ramos Paja, C.A., and Giral, R. (2016). Maximum power point tracking of photovoltaic systems based on the sliding mode control of the module admittance. *Electric Power Systems Research*, 136, 125–134.

Hamayun, M.T., Edwards, C., and Alwi, H. (2016). *Fault tolerant control schemes using integral sliding modes*, volume 61 of *Studies in Systems, Decision and Control*. Springer International Publishing Switzerland.

He, Y., Xu, W., and Cheng, Y. (2010). A novel scheme for sliding-mode control of dc-dc converters with a constant frequency based on the averaging model. *Journal of Power Electronics*, 10(1), 1–8.

Hung, J.Y., Gao, W., and Hung, J.C. (1993). Variable structure control: a survey. *IEEE Transactions on Industrial Electronics*, 40(1), 2–22.

Itkis, Y. (1976). *Control systems of variable structure*. New York: Wiley.

Khebbache, H. and Tadjine, M. (2013). Robust fuzzy backstepping sliding mode controller for a quadrotor unmanned aerial vehicle. *Journal of Control Engineering and Applied Informatics*, 15(2), 3–11.

Lee, H., Utkin, V., and Malinin, A. (2009). Chattering reduction using multiphase sliding mode control. *International Journal of Control*, 82(9), 1720–1737.

Leusink, D., Alfano, D., and Cinnella, P. (2015). Multifidelity optimization strategy for the industrial aerodynamic design of helicopter rotor blades. *Aerospace Science and Technology*, 42, 136–147.

Liu, R. and Li, S. (2014). Suboptimal integral sliding mode controller design for a class of affine systems. *Journal of Optimization Theory and Applications*, 161(3), 877–904.

Lopes, R.V., Galvao, R.K., Milhan, A.P., Becerra, V.M., and Yoneyama, T. (2006). Modelling and constrained predictive control of a 3dof helicopter. In *XVI Congresso Brasileiro de Automática*, volume 123, 429–434. Salvador, Brazil.

Martínez Marbán, E. (2015). *Modelado y control de un sistema aerodinámico angular*. Master's thesis, Universidad Autónoma del Estado de México - Facultad de Ingeniería.

Mueller, J.B., Paluszek, M.A., and Zhao, Y. (2004). Development of an aerodynamic model and control law design for a high altitude airship. In *AIAA 3rd "Unmanned Unlimited" Technical Conference, Workshop and Exhibit*.

Othman, S.M., Rahmat, M.F., Rozali, S., and Salleh, S. (2015). Review on sliding mode control and its application in electrohydrahulic acuator system. *Journal of Theoretical and Applied Information Technology*, 77(2), 199–208.

Piltan, F. and Sulaiman, N.B. (2012). Review of sliding mode control of robotic manipulator. *World Applied Sciences Journal*, 18(12), 1855–1869.

Pisano, A. and Usai, E. (2011). Sliding mde control: a survey with applications in math. *Mathematics and Computers in Simulation*, 81(5), 954–979.

Rekioua, D., Achour, A.Y., and Rekioua, T. (2013). Tracking power photovoltaic system with sliding mode control strategy. *Energy Procedia*, 36, 219–230.

Rossomando, F., Soria, C., and Carelli, R. (2014). Sliding mode control for trajectory tracking of a non-holonomic mobile robot using adaptive neural networks. *Journal of Control Engineering and Applied Informatics*, 16(1), 12–21.

Schreck, S.J. and Robinson, M.C. (2007). Horizontal axis wind turbine blade aerodynamics in experiments and modeling. *IEEE Transactions on Energy Conversion*, 22(1), 61–70.

Sefriti, S., Boumhidi, J., Naoual, R., and Boumhidi, I. (2012). Adaptive neural network sliding mode control for electrically-driven robot manipulators. *Journal of Control Engineering and Applied Informatics*, 14(4), 27–32.

Sira Ramírez, H. (2015). *Sliding mode control: the delta-sigma modulation approach*. Control Engineering. Birkhäuser Basel.

Tan, S., Lai, Y., Tse, C., and M.K.H., C. (2005). A fixed-frequency pulsewidth modulation based quasi-sliding-mode controller for buck converters. *IEEE Transactions on Power Electronics*, 20(6), 1379–1392.

Utkin, V. and Lee, H. (2006). Chattering problem in sliding mode control systems. In *Proceedings of the 2006 International Workshop on Variable Structure Systems*.

Utkin, V.I. (1977). Survey paper: Variable structure systems with sliding modes. *IEEE Transactions on Automatic Control*, 22(2), 212–22.

Utkin, V.I. (1978). *Sliding modes and their applications in variable structure systems*. Moscow: Mir.

Wu, L., Shi, P., and Su, X. (2014). *Sliding mode control of uncertain parameter-switching hybrid systems*. John Wiley & Sons.

Young, K.D., Utkin, V.I., and Özgüner, U. (1999). A control engineer's guide to sliding mode control. *IEEE Transactions on Control Systems Technology*, 7(3), 328–342.

Zhenga, E.H., Xiong, J.J., and Luo, J.L. (2014). Second order sliding mode control for a quadrotor uav. *ISA Transactions - Disturbance Estimation and Mitigation*, 53(4), 1350–1356.